Макрогетероциклы
http://macroheterocycles.isuct.ru

DOI: 10.6060/mhc161176p

Hybrid Materials of Zinc(II) Tetra−*tert*−butylphthalocyanine and Zinc(II) Tetra−*tert*−butylnaphthalocyanine with Single Walled Carbon Nanotubes: Structure and Sensing Properties

Maxim S. Polyakov[a@] and Tamara V. Basova[a,b]

[a]*Nikolaev Institute of Inorganic Chemistry, 630090 Novosibirsk, Russia*
[b]*Novosibirsk State University, 630090 Novosibirsk, Russia*
[@]*Corresponding author E-mail: maxpol@niic.nsc.ru*

The influence of extension of the aromatic core of phthalocyanines derivatives on the properties of the functionalized single walled carbon nanotubes (CNT) is studied. For this purpose the comparative study of the structural features and sensing properties of the CNT functionalized with zinc 2,9,16,23-tetra-tert-butylphthalocyanine (ZnPc) and zinc 2,11,20,29-tetra-tert-butyl-2,3-naphthalocyanine complex (ZnNc) is carried out. The adsorption of ZnPc and ZnNc molecules onto the CNT surface has been confirmed by Raman spectroscopy, SEM, and thermogravimetric analysis. It was determined that the number of ZnNc molecules anchored on the CNT walls is more than the number of ZnPc molecules. The more preferable π-π interaction of ZnNc molecules with CNT appears to be due to the bigger number of π-electrons forming naphthalocyanine aromatic system. Thin films of pristine CNT, CNT/ZnPc and CNT/ZnNc hybrids were prepared by drop casting onto interdigitated electrodes and applied as active layers to detect ammonia vapour (10-50 ppm) by measuring electrical resistance changes. It has been shown that sensor response of the CNT/ZnNc hybrid toward ammonia vapours is lager than that of CNT/ZnPc hybrid.

Keywords: Zinc phthalocyanine, zinc naphthalocyanine, carbon nanotubes, hybrid materials, chemical sensors.

Гибридные материалы на основе тетра−*трет*−бутилзамещённого фталоцианината и нафталоцианината цинка с одностенными углеродными нанотрубками: структура и сенсорные свойства

М. С. Поляков,[a@] Т. В. Басова[a,b]

[a]*Федеральное государственное бюджетное учреждение науки Институт неорганической химии им. А.В.Николаева Сибирского отделения Российской академии наук, 630090 Новосибирск, Россия*
[b]*Новосибирский государственный университет, 630090 Новосибирск, Россия*
[@]*E-mail: maxpol@niic.nsc.ru*

В работе рассмотрено влияние расширения π-системы производных фталоцианината цинка на свойства их гибридных материалов с одностенными углеродными нанотрубками (УНТ). С этой целью были исследованы структурные особенности и сенсорные свойства УНТ, функционализированных комплексами 2,9,16,23-тетра-трет-бутилнафталоцианината цинка (ZnNc) и 2,11,20,29-тетра-трет-бутилфталоцианината цинка (ZnPc). Адсорбция молекул ZnNc и ZnPc на поверхность углеродных нанотрубок подтверждалась методами КР-спектроскопии, сканирующей электронной микроскопии и термогравиметрии. Определено, что количество молекул ZnNc, адсорбированных на поверхности УНТ, в два раза превышает количество молекул ZnPc. Более предпочтительное π-π-взаимодействие между ZnNc и УНТ можно объяснить большим числом π-электронов, участвующих в формировании ароматической системы нафталоцианина. Тонкие плёнки УНТ, УНТ/ZnPc, УНТ/ZnNc осаждались на подложки со встречно-штыревыми электродами капельным методом. Полученные плёнки были протестированы в качестве активных слоёв сенсоров на пары аммиака (10-50 ppm). Посредством

измерения резистивного отклика показано, что сенсорный отклик плёнки гибридного материала УНТ/ZnNc на пары аммиака больше по сравнению с плёнкой на основе УНТ/ZnPc.

Ключевые слова: Фталоцианинат цинка, нафталоцианинат цинка, углеродные трубки, гибридные материалы, химические сенсоры.

Introduction

Phthalocyanine and its metal complexes are known to be useful in the wide range of applications as dyes, pigments, photosensitizers, active layers of optical discs, sensors, solar cells, *etc*.[1,2] due to their versatile properties coming from their π-conjugated structure. Phthalocyanine properties can be tuned both by changing central metals and by introduction of different substituents into the aromatic ring.[3,4] Due to their semiconductor properties metal phthalocyanines are used as resistive sensors toward different gases and volatile organic compounds (VOCs).[5,6] For instance, it is well known that phthalocyanines have significant potential to be used as active layers of sensors for detection of NH_3 and amines,[7-9] as well as many other gases, namely NO_x,[10-12] CO,[13,14] H_2,[15,16] H_2S and thiol[17] vapours.

Besides some useful properties as active sensor layers phthalocyanine films have some disadvantages associated with their comparatively low conductivity and poor mechanical properties. One of the manners to overcome these obstacles is preparation of the hybrid materials on the basis of phthalocyanines and carbon nanomaterials (CNT or graphene). Combination of the properties of CNT (high conductivity and extremely high surface area) and the properties of MPc derivatives (appropriate binding sites for analytes resulting in charge transfer complexes) provides grounds for synergetic effect between CNTs and metal phthalocyanines. The CNT hybrids therefore provide good prospect for sensor applications as it has already been demonstrated in previous publications.[18-21] Wang *et al.* have immobilized tetra-*tert*-butylphthalocyanine on carbon nanotubes by π-π-interaction.[22] To enhance π-π interaction between MPc molecule and CNT surface and, therefore, to increase adsorption of phthalocyanines, introduction of aromatic substituents into the macroring was suggested. Pyrene groups were assumed to interact strongly with CNTs *via* π-π interaction.[23-25] Torres *et al*.[24] used metal and metal-free pyrene substituted phthalocyanines to form stable electron donor-acceptor hybrids. In our recent publication, we compared the structural features and sensor properties of hybrids of single walled carbon nanotubes with symmetrically polyoxyethylene octasubstituted ZnPc and similar asymmetrically substituted ZnPc-py with one pyrene group as a substituent.[26] It was shown that the interaction of ZnPc-py with CNTs is more favourable than in the case of ZnPc without pyrene substituents and the sensor response of ZnPc-py hybrid toward ammonia was larger.

In the present work, the influence of extension of the aromatic core on the properties of the functionalized single walled carbon nanotubes (CNT) is studied. For this purpose the comparative study of the structural features and sensing properties of the CNTs functionalized with zinc 2,9,16,23-tetra-*tert*-butylphthalocyanine (ZnPc) and zinc 2,11,20,29-tetra-*tert*-butyl-2,3-naphthalocyanine complex (ZnNc) is carried out. It is suggested that the additional benzene rings in ZnNc molecule will improve π-π interactions between naphthalocyanine aromatic ring and CNT surface.

Some properties of the hybrid materials on the basis of CNT and MNc have already been described elsewhere.[27-29] The photoconductivity of the hybrid films was found to increase remarkably in the visible region and broaden towards the red region.[29] The sensing properties of CNT/MNc hybrids have not been discussed in the literature.

Experimental

Materials

The methods of the synthesis and purification of zinc 2,9,16,23-tetra-*tert*-butylphthalocyanine (ZnPc) have already been published elsewhere.[30,31] Zinc 2,11,20,29-tetra-*tert*-butyl-2,3-naphthalocyanine (ZnNc) was purchased from Sigma-Aldrich (95 %) and purified by column chromatography (silica gel). CNTs were purchased from Sigma-Aldrich and used without further purification or chemical treatment.

Equipment

Shimadzu UV-Vis-3101 spectrometer was used for registration of the absorption spectra in the UV-visible region at room temperature. Scanning electron microscopy (SEM) images were obtained using a FEI-nova nanosem 200 instrument at an accelerating voltage of 5 kV. A Triplemate, SPEX spectrometer equipped with CCD detector was used for detection of Raman spectra in back-scattering geometry. An Ar-laser (488 nm, 40 mW) was used for the spectral excitation.

Thermogravimetric analysis (TGA) was carried out using a NETZSCH TG 209 F1 at a rate of 10 °C·min^{-1} in a helium flow (30 mL·min^{-1}). The films thickness was measured using spectroscopic ellipsometry (Woolam M2000VTM rotating analyser spectroscopic ellipsometer). Transmission electron microscopy (TEM) images were obtained using JEM-2010 instrument at an accelerating voltage of 200 kV. DC-conductivity measurements were carried out using Keithley 236 semiconductors characterization system.

Preparation of CNT/ZnPc and CNT/ZnNc Hybrids

ZnPc (5 mg) and ZnNc (5 mg) solutions were prepared by dissolving in 1 mL DMF and then sonicated for 15 minutes. Single walled carbon nanotubes were added to 3 mL of DMF and then their suspension was subjected to sonication for 30 minutes. To obtain the CNT/ZnPc and CNT/ZnNc hybrids, the solution of ZnPc and ZnNc was dropped to the CNTs suspension, respectively. Addition of the solution was continued until the solution colour is discoloured caused by adsorption of the phthalocyanine onto the CNT surface. After stirring for another hour the mixture was centrifuged, and the

obtained precipitate was washed with DMF several times, once with CH_2Cl_2, then centrifuged again and dried in vacuum.

Sensor Properties Study

The sensor response to low-concentration of NH_3 in the range 10–50 ppm was studied. Pure commercial NH_3 gas ("Dioksid", Russia) was used as the NH_3 source. Argon was used as a diluting and purging gas. Concentration and flow of NH_3 and Ar were controlled using mass flow controllers. The relative humidity was about 50 %.

Pristine ZnPc, ZnNc or their CNT/ZnPc and CNT/ZnNc hybrids were obtained as thin films by spin-coating their solutions in dichloromethane on glass substrates with deposited interdigitated Pt electrodes (DropSens, G-IDEPT10). The dimension of gaps was 10 μm; the number of digits was 125×2 with a digit length equal to 6760 μm; cell constant is 0.0118 cm^{-1}. The electrical characterization of the hybrid films was carried out using a Keithley 236 electrometer by applying a constant dc voltage of 3 V.

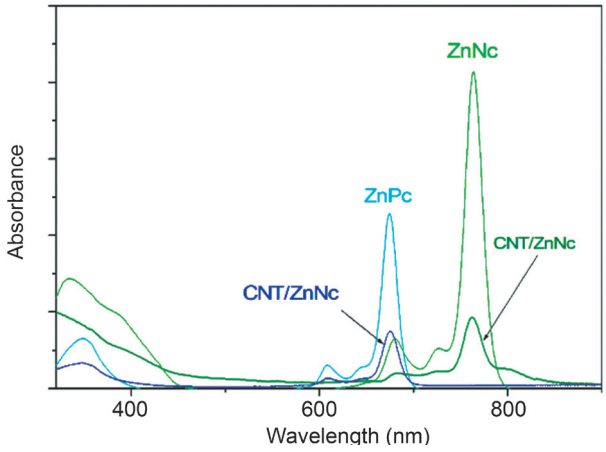

Figure 1. UV–Visible absorption spectra of ZnPc, ZnNc and their hybrid materials (CNT/ZnPc and CNT/ZnNc) dispersed in DMF.

Results and Discussion

Spectral Study

The optical absorption spectra of ZnPc and ZnNc solutions and their hybrids in DMF are shown in Figure 1. The phthalocyanines are soluble in DMF while their hybrids exhibit good dispersion in this solvent. The Q-band of ZnPc in DMF is located at 674 nm, while the Q-band of ZnNc is shifted to the near-infrared region and centered at 763 nm. In both cases the Q-bands are attributed to the π-π* transition from the highest occupied molecular orbital (HOMO) to the lowest unoccupied molecular orbital (LUMO) of the aromatic ring.[32] Both ZnPc and ZnNc exist in the solutions in a monomeric form, as evidenced by the narrow Q-bands in the electronic absorption spectra.[33] The CNTs with sufficient electron delocalization act as the favorable adsorption sites for ZnNc. ZnNc molecules are adsorbed on the CNT surface via the π-π interactions to form the CNT/ZnNc hybrid. Both CNT/ZnPc and CNT/ZnNc hybrids are characterized by broadened absorption peaks with lowered intensities. Similar absorption spectra were demonstrated for ZnPc adsorbed on the surface of graphene composite by Karousis *et al.*;[34] they have revealed that such spectra give obvious indication of ground-state electronic interactions between ZnPc and graphene within the hybrid materials.

Microscopic Study

Indirect evidence for CNT/ZnPc and CNT/ZnNc interactions can be reached from scanning electron microscopy. Inspecting the SEM images of pristine CNT shows the presence of large bundles of nanotubes. Figure 2 shows SEM images of pristine CNT (a) and CNT/ZnNc hybrid (b) as powders. Compared to the pristine CNT (Figure 2a), the SEM images of CNT/ZnNc hybrid show the observable increase of the thickness of CNT bundles, confirming the formation of nanohybrids, probably due to π–π interactions between the phthalocyanine and CNT. After CNT functionalization with ZnNc, nanoparticles of ZnNc with a diameter from several to tens of nanometers are clearly resolved on CNT walls. Figure 2b obviously shows the bundles of nanotubes in the hybrid and the clusters of phthalocyanine attached on the surfaces of CNTs.

The non-covalent functionalization of CNT with ZnPc was also confirmed by Raman spectroscopy. The Raman

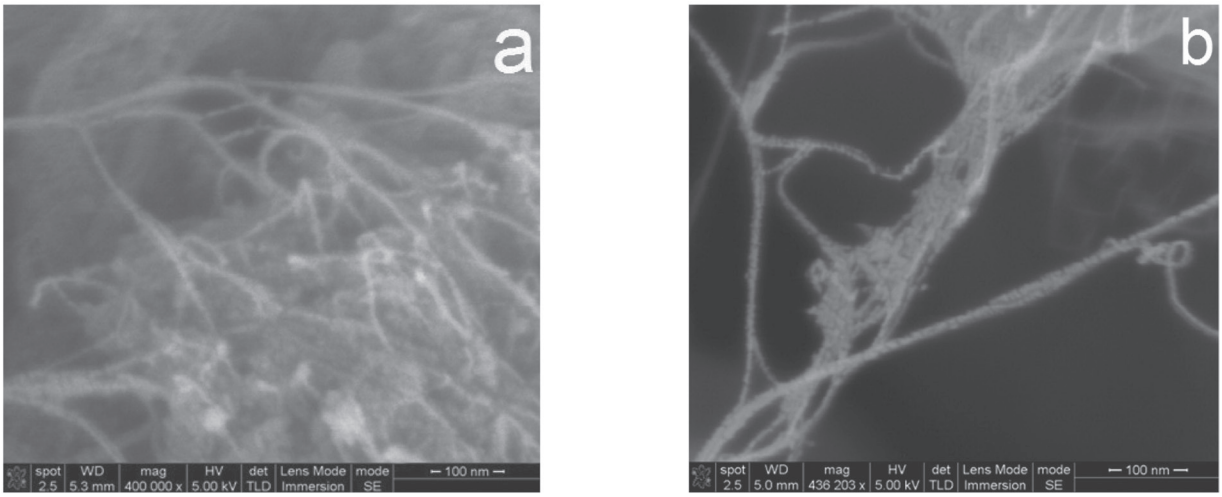

Figure 2. SEM images of (a) pristine CNT and (b) CNT/ZnNc hybrid.

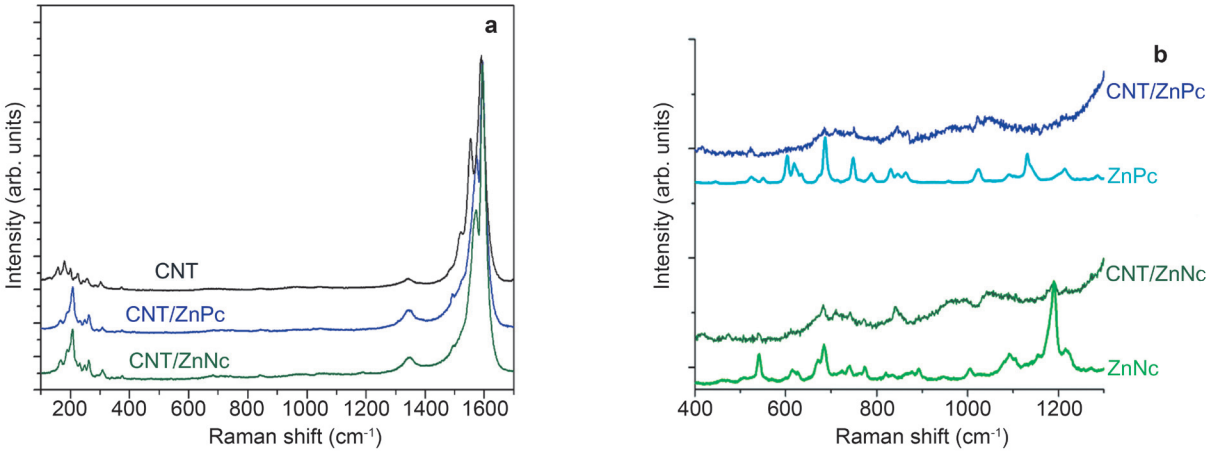

Figure 3. (a) Raman spectra of pristine CNT, CNT/ZnPc and CNT/ZnNc hybrids in the range 90–1700 cm^{-1}. (b) Raman spectra of the pure ZnPc and ZnNc as well as their hybrids in the range 400–1300 cm^{-1}.

spectra of the hybrids were compared to that of pristine CNTs (Figure 3a). The ratio of intensities of the radial breathing modes (RBM), disorder (D) mode and graphite (G) mode are used to monitor functionalization with the phthalocyanines.[35-39] The spectra were normalized to the graphite G-band at ~1590 cm^{-1}. The spectra of both CNT and CNT/MPc hybrids contain the typical disorder mode D at about 1340 cm^{-1}, and the G band at 1590 cm^{-1}.

The ratio of the D band to the G band (I_D/I_G) has a value of 0.016 in the spectrum of pure CNT, while the values of 0.027 and 0.021 are observed in the spectra of the hybrids with ZnPc and ZnNc, respectively. This small variation of the I_D/I_G ratio suggests that ZnPc and ZnNc derivatives are attached to the surface of CNT through non-covalent bonding. Figure 3b shows the enlarged section of the Raman spectrum from 400 to 1300 cm^{-1}, showing the characteristic vibrations of phthalocyanine macrocycle. The bands corresponding to Pc macrocycle are noticeable in the spectrum of both CNT/ZnPc and CNT/ZnNc. Comparison of the hybrids' spectra with those of pure ZnPc and ZnNc (Figure 3b) shows that some characteristic vibrations of phthalocyanine macrocycle were noticeably shifted due to interaction with CNT.

The RBMs of CNT in the range of 156–310 cm^{-1} (Figure 2a) correspond to a distribution of CNT diameters in the range from 0.7 to 1.4 nm.[40,41] Noticeable shifts in the RBM positions were observed. The RBMs at 156, 179, 200, 223, 243, 257, 303 cm^{-1} of CNT are shifted to 165, 186, 206, 232, 248, 263, 308 cm^{-1} after the adsorption of ZnPc, and to 165, 188, 206, 231, 247, 262, 309 cm^{-1} after the adsorption of ZnNc. The sensitivity of RBMs to the adsorption of polynuclear aromatic macrocycles by carbon nanotubes was demonstrated by Gotovac *et al*.[42] The π-π stacking interaction between carbon nanotube walls and the MPc core gives rise a shift to a higher frequency range due to the "hardening effect" described by Zhang *et al*.[43]

TG Analysis

To estimate the amount of ZnPc and ZnNc molecules adsorbed on CNT surface TG analysis was carried out. Figure 4 shows the weight loss of about 10.7 % in the case of pristine CNTs at 600 °C. It has also been revealed that the thermograms of ZnPc (Figure 4) and ZnNc (Figure 5) present a loss of weight of 29.1 % and 28.3 %, respectively. A weight loss of 16.3 % and 21.5 % was registered in the TGA experiment upon heating of hybrids to 600 °C in the inert atmosphere for CNT/ZnPc and CNT/ZnNc, respectively. Taking into account the CNT weight loss, the corrected weight loss of the hybrids due to ZnPc or ZnNc adsorption on the CNT surface was calculated to be 5.6 % for ZnPc and 10.8 % for ZnNc. Concerning the number of phthalocyanines/naphthalocyanine molecules adsorbed on CNTs, the ratios of the ZnPc and ZnNc weight loss have been estimated as 19.2 % (5.6 %/29.1 %) for ZnPc and 38.1 % (10.8 %/28.3 %) for ZnNc. As a result, the number of carbon atoms per one molecule of ZnPc or ZnNc was estimated to be 280 [(80.8 %×802.34)/(19.2 %×12)] and 157 [(71.9 %×1002.58)/(38.1 %×12)], respectively.

As a result, the number of ZnNc molecules anchored on the CNT walls is more than the number of ZnPc molecules. The more preferable p-p interaction of ZnNc molecules with CNT appears to be due to the larger number of p-electrons

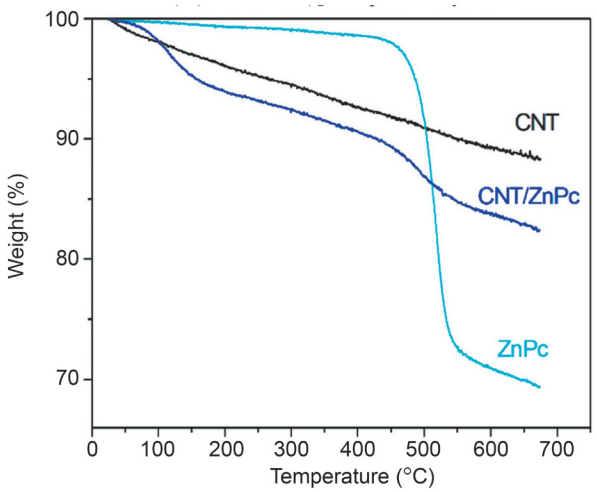

Figure 4. Thermogravimetric analysis (TGA) of bare CNT, ZnPc and CNT/ZnPc hybrid.

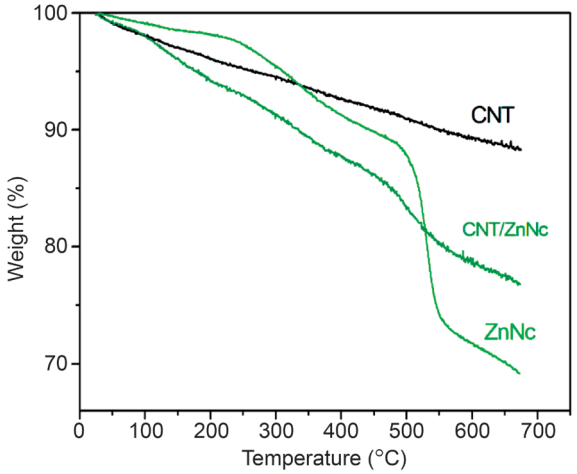

Figure 5. Thermogravimetric analysis (TGA) of bare CNT, ZnNc and CNT/ZnNc hybrid.

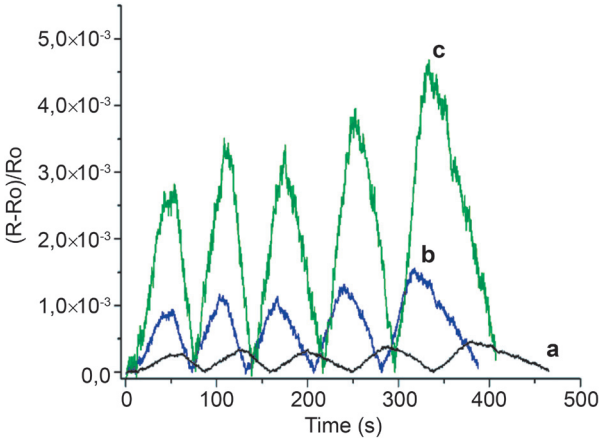

Figure 6. Normalized sensor response of the sensor layers of CNT (a), CNT/ZnPc (b) and CNT/ZnNc hybrids (c).

forming naphthalocyanine aromatic system. Similar results were obtained by E. Kaya *et al.*;[26] it was shown that the number of ZnPc molecules containing aromatic pyren substituent is more than that of similar ZnPc derivative without pyren.

Study of sensing properties of CNT/ZnPc and CNT/ZnNc hybrids

Thin films of CNTs and their hybrids with ZnPc and ZnNc were spun onto interdigitated electrodes in order to investigate their sensing properties. The average thickness of the investigated films was 10–15 nm. Figure 6 shows the normalized sensor response R ($R=(R-R_o)/R_o$, where R is the film resistance at the detected concentration of an analyte and R_o is the baseline resistance) of the sensor layers of CNT/ZnPc and CNT/ZnNc hybrids as well as pristine CNT on exposure to 10, 20, 30, 40 and 50 ppm of NH_3. The resistance of the obtained films increases as a result of adsorption of the electron donating NH_3 molecules, leading to charge transfer between the hybrid film and NH_3 molecules. This result shows that the hybrids exhibit p-type conductivity behaviour. All studied sensors demonstrate a reversible response. The recovery time of CNT/ZnPc and CNT/ZnNc hybrids is 30 and 40 s, respectively, while that of pristine CNT is 60–80 s. The studied hybrids exhibit more stable and reproducible response upon exposure to NH_3 compared to that of pristine CNT films.

Figure 7 demonstrates the dependence of the relative sensor responses of CNT/ZnPc, CNT/ZnNc hybrids and pristine CNT on the NH_3 concentrations. It is obvious that the sensor response of both hybrids is higher than that of pristine CNT.

It has already been shown elsewhere[44] that surface charge transfer interaction occurs upon adsorption of strong electron donor molecules like ammonia onto the surface of phthalocyanine derivative in their hybrids with carbon nanomaterials. The electrons transfer from NH_3 to a phthalocyanine molecule; the formed charge-transfer complexes trap holes leading to increase of the resistance. Since CNT/MPc conjugates can form an excellent charge

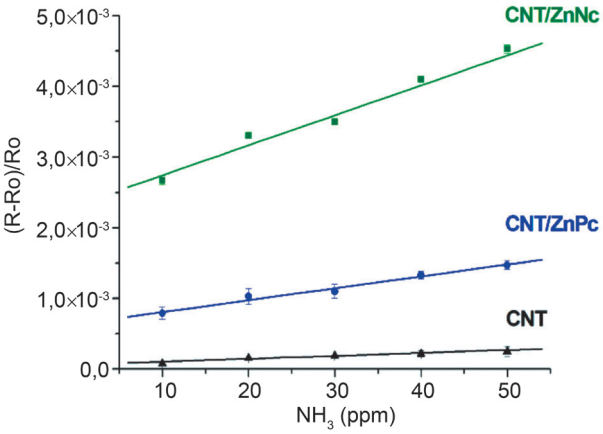

Figure 7. Dependence of the normalized sensor response of CNT(a), CNT/ZnPc and CNT/ZnNc hybrids on ammonia concentration.

transfer complexes,[45] the charge can favourably travel from MPc derivatives to CNTs rapidly, resulting in a large and fast variation of the resistance. The combination of the useful properties of CNT (namely, high conductivity and extremely high surface area), and the properties of MPc derivatives (namely, appropriate binding sites for ammonia resulting in charge transfer complexes) provides grounds for synergetic effect between CNTs and ZnPc (or ZnNc) derivatives as active layers for sensor applications.

It is necessary to mention that the CNT/ZnNc hybrid has higher response in comparison with CNT/ZnPc, that is in good correlation with the number of molecules adsorbed onto the CNT wall, as estimated by TGA (Figures 4 and 5). The more MPc molecules are adsorbed on CNT surface, the larger sensor response is observed.

Conclusions

Hybrid structures of single-walled carbon nanotubes with zinc 2,9,16,23-tetra-*tert*-butylphthalocyanine (ZnPc)

and zinc 2,11,20,29-tetra-*tert*-butyl-2,3-naphthalocyanine (ZnNc) have been prepared and characterized by spectral methods and microscopy. It was shown by the methods of Raman spectroscopy and thermogravimetry that ZnNc interacts with CNT more efficiently than ZnPc. The amount of ZnNc anchored on the surface of nanotubes is almost 1.8 times more than ZnPc. To demonstrate the potential applications of the CNT/ZnPc and CNT/ZnNc hybrids towards gas sensing, a resistive gas sensor device based on the hybrid materials has been fabricated. The comparative analysis of sensor response of pristine CNT films and hybrid films to ammonia vapour (10–50 ppm) was carried out to demonstrate the synergetic effect between CNTs and the phthalocyanine derivatives. It was shown that the sensor response of both hybrids is higher than that of pristine CNT. At the same time the response of the films of CNT/ZnNc hybrid to the ammonia vapour is about 3 times larger than that of the films of CNT/ZnPc hybrid.

Acknowledgements This work was supported by the Russian Science Foundation (project № 15-13-10014).

References

1. Dini D., Hanack M. Physical Properties of Phthalocyanine-based Materials. In: *The Porphyrin Handbook. Phthalocyanines: Properties and Materials* (Kadish K.M., Kevin K.M., Smith R., Eds.) San Diego: Academic Press, **2003**. p. 1–140.
2. Hughes S., Spruce G., Wherrett B.S., Kobayashi T. *J. Appl. Phys.* **1997**, *81*, 5905–5912.
3. Kouzeki T., Tatezono S., Yanagi H. *J. Phys. Chem.* **1996**, *100*, 20097–20102.
4. Yanagi H., Kanbayashi Y., Schlettwein D., Woehrle D., Armstrong N.R. *J. Phys. Chem.* **1994**, *98*, 4760–4766.
5. Basova T.V., Hassan A., Krasnov P.O., Gürol I., Ahsen V. *Sens. Actuators, B* **2015**, *216*, 204–211.
6. Gao L.D., Qian X.H. *J. Fluor. Chem.* **2002**, *113*, 161–165.
7. Wang B., Wu Y., Wang X., Chen Z., He C. *Sens. Actuators, B* **2014**, *190*, 157–164.
8. Jiang D.P., Lu A.D., Li Y.J., Pang X.M., Hua Y.L. *Thin Solid Films* **1991**, *199*, 173–179.
9. Chicharro M., Zapardiel A., Bermejo E. *Anal. Bioanal. Chem.* **2002**, *373*, 277–283.
10. Fernandez-Sanchez J.F., Nezel T., Steiger R., Spichiger-Keller U.E. *Sens. Actuators, B* **2006**, *113*, 630–638.
11. Chakane S., Gokarna A., Bhoraskar S.V. *Sens. Actuators, B* **2003**, *92*, 1–5.
12. Zhao L., Zhu S., Zhou J. *Sens. Actuators, B* **2012**, *171*, 563–571.
13. Fernandez-Sanchez J.F., Fernandez I., Steiger R., Beer R., Cannas R., Spichiger-Keller U.E. *Adv. Funct. Mater.* **2007**, *17*, 1188–1198.
14. Viricelle J.P., Pauly A., Mazet L., Brunet J., Bouvet M., Varenne C., Pijolat C. *Mater. Sci. Eng. C* **2006**, *26*, 186–195.
15. Uwira V., Schutze A., Kohl D. *Sens. Actuators, B* **1995**, *26*, 153–157.
16. Jakubik W., Urbanczyk M., Maciak E. *Sens. Actuators, B* **2007**, *127*, 295–303.
17. Argote M.R., Guillen E.S., Porras A.G.G., Torres O.S., Richard C., Zagal J.H., Bedioui F., Granados S.G., Griveau S. *Electroanal.* **2014**, *26*, 507–512.
18. Feng X., Irle S., Witek H., Morokuma K., Vidic R., Borguet E.J. *J. Am. Chem. Soc.* **2005**, *127*, 10533–10538.
19. Lucci M., Reale A., Carlo D.A., Orlanducci S., Tamburri E., Terranova M.L., Davolic I., Di Natale C., D'Amicoa A., Paolesse R. *Sens. Actuators, B* **2006**, *118*, 226–231.
20. Alwarappan S., Liu G., Li C. Z. *Nanomedicine: Nanotechnol., Biology Medicine* **2010**, *6*, 52–57.
21. Jyothirmayee Aravind S.S., Ramaprabhu S. *Sens. Actuators, B* **2011**, *155*, 679-686.
22. Wang X., Liu Y., Qiu W., Zhu D. *J. Mater. Chem.* **2002**, *12*, 1636–1639.
23. Bogani L., Danieli C., Biavardi E., Bendiab N., Barra A.L., Dalcanale E., Wernsdorfer W., Cornia A. *Angew. Chem., Int. Ed.* **2009**, *48*, 746–750.
24. Bartelmess J., Ballesteros B., de la Torre G., Kiessling D., Campidelli S., Prato M., Torres T., Guldi D.M. *J. Am. Chem. Soc.* **2010**, *132*, 16202–16211.
25. Ogbodu R.O., Antunes E., Nyokong T. *Dalton Trans.* **2013**, *42*, 10769–10777.
26. Kaya E.N., Tuncel S., Basova T.V., Banimuslem H., Hassan A., Gürek A.G., Ahsen V., Durmuş M. *Sens. Actuators, B* **2014**, *199*, 277–283.
27. Zhang X., Feng Y., Tang S., Feng W. *Carbon* **2010**, *48*, 211–216.
28. Feng Y., Zhang X., Feng W. *Organic Electronics* **2010**, *11*, 1016–1019.
29. Feng W., Li Y., Feng Y., Wu J. *Nanotechnology* **2006**, *17*, 3274–3279.
30. Lebedeva N.Sh., Pavlycheva N.A., Parfenuk E.V., Vyugin A.I. J. Chem. *Thermodynamics* **2006**, *38(2)*, 165–172.
31. Janczak J., Kubiak R. *Polyhedron* **2001**, *20*, 2901–2909.
32. Ceyhan T., Altindal A., Özkaya A.R., Çelikbiçak Ö., Salih B., Kemal Erbil M., Bekaroğlu Ö. *Polyhedron* **2007**, *26*, 4239–4249.
33. Durmus M., Nyokong T. *Polyhedron* **2007**, *26*, 2767–2776.
34. Karousis N., Ortiz J., Ohkubo K., Hasobe T., Fukuzumi S., Sastre-Santos A., Tagmatarchis N. *J. Phys. Chem. C* **2012**, *116*, 20564–20573.
35. Wepasnick K.A., Smith B.A., Bitter J.L. *Anal. Bioanal. Chem.* **2010**, *396*, 1003-1014.
36. Mugadza T., Nyokong T. *Electrochim. Acta* **2010**, *55*, 6049–6057.
37. Ballesteros B., de la Torre G., Ehli C., Rahman G.M.A., Rueda F., Guidi D.M., Torres T. *J. Am. Chem. Soc.* **2007**, *129*, 5061–5068.
38. Casiraghi C., Hartschuh A., Qian H., Pliscanec S., Georgia C., Fasoli A., Novoselov K.S., Basko D.M., Ferrari A.C. *Nano Lett.* **2009**, *9*, 1433–1441.
39. Dyke C., Tour J. *Nano Lett.* **2003**, *3*, 1215–1218.
40. Alvarez L., De la Fuente G., Righi A., Rols S., Anglaret E., Sauvajol J., Munoz E., Maser W., Benito A., Martinez M. *Phys. Rev. B* **2001**, *63*, 153401.
41. Huo D., Yang L., Hou C., Fa H., Luo X., Lu Y., Zheng X., Yang J., Yang L. *Spectrochim. Acta, Part A* **2009**, *74*, 336–343.
42. Gotovac S., Honda H., Hattori Y., Takahashi K., Kanoh H., Kaneko K. *Nano Lett.* **2007**, *7*, 583–587.
43. Zhang Y., Zhang J., Son H., Kong J., Liu Z. *J. Am. Chem. Soc.* **2005**, *127*, 17156–17157.
44. Wang B., Zhou X., Wu Y., Chen Z., He C., Zuo X. *Sens. Actuators, B* **2012**, *161*, 498–503.
45. Chidawanyika W., Nyokong T. *Carbon* **2010**, *48*, 2831–2838.

Received 09.11.2016
Accepted 01.03.2017